How to cite: *Angew. Chem. Int. Ed.* **2024**, *63*, e202319658
doi.org/10.1002/anie.202319658

VIP Polymer Chemistry Very Important Paper

Cyano-Functionalized Pyrazine: A Structurally Simple and Easily Accessible Electron-Deficient Building Block for n-Type Organic Thermoelectric Polymers

*Lijun Tu[+], Junwei Wang[+], Ziang Wu, Jianfeng Li, Wanli Yang, Bin Liu, Siqi Wu, Xiaomin Xia, Yimei Wang, Han Young Woo, and Yongqiang Shi**

Abstract: Developing low-cost and high-performance n-type polymer semiconductors is essential to accelerate the application of organic thermoelectrics (OTEs). To achieve this objective, it is critical to design strong electron-deficient building blocks with simple structure and easy synthesis, which are essential for the development of n-type polymer semiconductors. Herein, we synthesized two cyano-functionalized highly electron-deficient building blocks, namely 3,6-dibromopyrazine-2-carbonitrile (CNPz) and 3,6-Dibromopyrazine-2,5-dicarbonitrile (DCNPz), which feature simple structures and facile synthesis. CNPz and DCNPz can be obtained via only one-step reaction and three-step reactions from cheap raw materials, respectively. Based on CNPz and DCNPz, two acceptor–acceptor (A–A) polymers, P(DPP-CNPz) and P(DPP-DCNPz) are successfully developed, featuring deep-positioned lowest unoccupied molecular orbital (LUMO) energy levels, which are beneficial to n-type organic thin-film transistors (OTFTs) and OTEs performance. An optimal unipolar electron mobility of 0.85 and 1.85 $cm^2V^{-1}s^{-1}$ is obtained for P(DPP-CNPz) and P(DPP-DCNPz), respectively. When doped with *N*-DMBI, P(DPP-CNPz) and P(DPP-DCNPz) show high n-type electrical conductivities/power factors of 25.3 $S\,cm^{-1}$/41.4 $\mu W\,m^{-1}K^{-2}$, and 33.9 $S\,cm^{-1}$/30.4 $\mu W\,m^{-1}K^{-2}$, respectively. Hence, the cyano-functionalized pyrazine CNPz and DCNPz represent a new class of structurally simple, low-cost and readily accessible electron-deficient building block for constructing n-type polymer semiconductors.

[*] L. Tu,[+] S. Wu, X. Xia, Prof. Y. Shi
Key Laboratory of Functional Molecular Solids, Ministry of Education, School of Chemistry and Materials Science, Anhui Normal University
No.189, Jiuhua South Road, Wuhu, Anhui, 241002, China
E-mail: shiyq@ahnu.edu.cn

J. Wang,[+] J. Li, W. Yang, B. Liu, Y. Wang
Department of Materials Science and Engineering, Southern University of Science and Technology (SUSTech)
Shenzhen, Guangdong 518055, China

Z. Wu, Prof. H. Y. Woo
Department of Chemistry, College of Science, Korea University
145 Anam-ro, Seongbuk-gu, Seoul 136-713, Korea

[+] These authors contributed equally to this work.

Introduction

Design and synthesis of novel π-conjugated building blocks is a powerful strategy to modulate the optoelectronic properties of organic semiconductors for advancing the field of organic electronics, such as organic thin-film transistors (OTFTs),[1] organic solar cells (OSCs),[2] perovskite solar cells (PVSCs),[3] and organic thermoelectrics (OTEs).[4] For instance, OTFTs have achieved excellent mobilities over 10 $cm^2V^{-1}s^{-1}$ and OSCs have demonstrated high power conversion efficiency (PCE) of over 19 %.[5] Although this strategy has been widely utilized to enrich the structural diversity of organic semiconductors, only a handful of n-type (electron-transporting) polymer semiconductors have shown exceptional device performance in the field, specifically in OTEs.[6]

For building efficient thermoelectric generators, high-performance complementary p-type (hole-transporting) and n-type (electron-transporting) semiconductors are both required. Up to now, p-type semiconducting polymers exhibit excellent TE performance with electrical conductivity (σ) over 2000 $S\,cm^{-1}$.[7] Nonetheless, there are only a limited number of n-type semiconducting polymers with σ over 10 $S\,cm^{-1}$.[8] The unbalanced development between n-type and p-type polymers restricted OTE materials practical applications.[9] Therefore, it is highly desired to develop n-type polymer semiconductors with high electrical conductivities. Notably, there are significant obstacles to overcome in order to develop high-performance n-type polymer semiconductors: Firstly, a deep-lying lowest unoccupied molecular orbital (LUMO) energy level of polymers is required for efficient electron transport, thus strong electron-withdrawing functional groups such as imide,[10] amide,[11] cyano,[12] or B←N groups[13] should be incorporated into the polymer backbone. Secondly, tuning of the polymer backbone from a donor–acceptor (D–A) type to an acceptor–acceptor (A–A) type is a power strategy to achieve unipolar n-type characteristics.[14] However, functional groups (trialkyltin or boronic ester) in electron-deficient monomers are required, which face huge challenges to synthesis and purification of these monomers. The availability of electron-deficient building blocks is limited, thus severely restricting the further development of high-performance n-type polymer semiconductors. Some representative strong electron-withdrawing building blocks have been reported in literatures, such as naphthalene diimide (NDI),[15] naphtho[2,3-

b:6,7-*b*′]-dithiophenediimide (NDTI),[16] bithiophene imide and derivatives (BTIn),[10a] benzodifurandione-based oligo(p-phenylene vinylene) (BDOPV),[17] B←N bridged bipyridine (BNBP),[13b] and diketopyrrolopyrrole (DPP) and derivatives.[18] These electron-deficient building blocks have been widely investigated for constructing high-performance n-type polymer semiconductors. For example, Guo et al. reported a CNI electron-deficient building blocks by introducing CN group onto BTI (Figure 1a), the CNI-based polymer shows a μ_e of 0.18 $cm^2V^{-1}s^{-1}$ and n-type σ of 23.3 Scm^{-1}.[19] Lei et al.[20] developed an n-type semiconducting polymer based on pyrazine-flanked DPP unit PzDPP (Figure 1a). Introduction of pyrazine electron-deficient building block into polymer backbone can effectively lower the LUMO energy level, tune the conjugated structure and intermolecular interaction of organic semiconductors, thus achieving high TE performance with PF of 57.3 $\mu W m^{-1}K^{-2}$. Geng et al. reported an n-type conjugated polymer based on thiazole-flanked DPP unit Tz-5-DPP (Figure 1a). Homopolymer PTz-5-DPP has low-lying HOMO and LUMO levels and shows great polaron delocalization. When doped with *N*-DMBI, PTz-5-DPP exhibited a σ of 8 Scm^{-1} and a PF as high as 106 $\mu W m^{-1}K^{-2}$.[18]

However, despite these building blocks and resulting polymers exhibiting excellent device performance, these electron acceptor units possess complicated chemical structures, lengthy synthetic route and tedious purification processes, thus resulting in increased production cost, which seriously limits their practical application in OTE. Furthermore, further modification of these monomers is remarkably challenging. Recently, decorating n-type semiconducting polymers with polar oligo (ethylene glycol) (OEG) side chain has drawn intensive attention for application in OTEs.[21] The introduction of polar side chains can increase the miscibility between host polymer and guest dopants, thus improving the TE performance. However, OEG side chains often bring unexpected low electron mobility and poor film morphology. Moreover, the OEG-monomer possesses tedious synthesis steps and needs multiple purifications, inevitably leading to high cost and low yield.[22]

Currently, many efforts are focused on improving thermoelectric performance, however, very few have been made to reduce the costs of the thermoelectric materials, and the costs of the efficient thermoelectric materials reported so far were too high to meet commercial application of the OTE due to their complicated molecular structures, verbose multi-steps synthesis, and multiple purifications.[23] Therefore, there is an urgent need to develop low-cost and efficient OTE materials to meet the basic requirements of OTE generators for the transition from the laboratory to commercialization. Herein, we design and synthesize two cyano-functionalized pyrazine electron-deficient building blocks, 3,6-dibromopyrazine-2-carbonitrile (CNPz) and 3,6-Dibromopyrazine-2,5-dicarbonitrile (DCNPz) (Figure 1b), which combine the advantages of both cyano and pyrazine functionalities to enable these two acceptors with strong electron-withdrawing characteristics, small steric hindrance, and planar backbone. CNPz and DCNPz possess simple molecular structures and can be synthesized with low cost and high yields. Notably, the synthesis of CNPz and DCNPz electron-deficient units requires only one-step reaction and three-step reactions from cheap raw materials, respectively. These CN-functionalized pyrazine units show deep-lying FMO and are much stronger electron acceptor units than imide, amide, and B←N units. Such strong acceptor units are highly pursued for developing n-type polymer semiconductors.

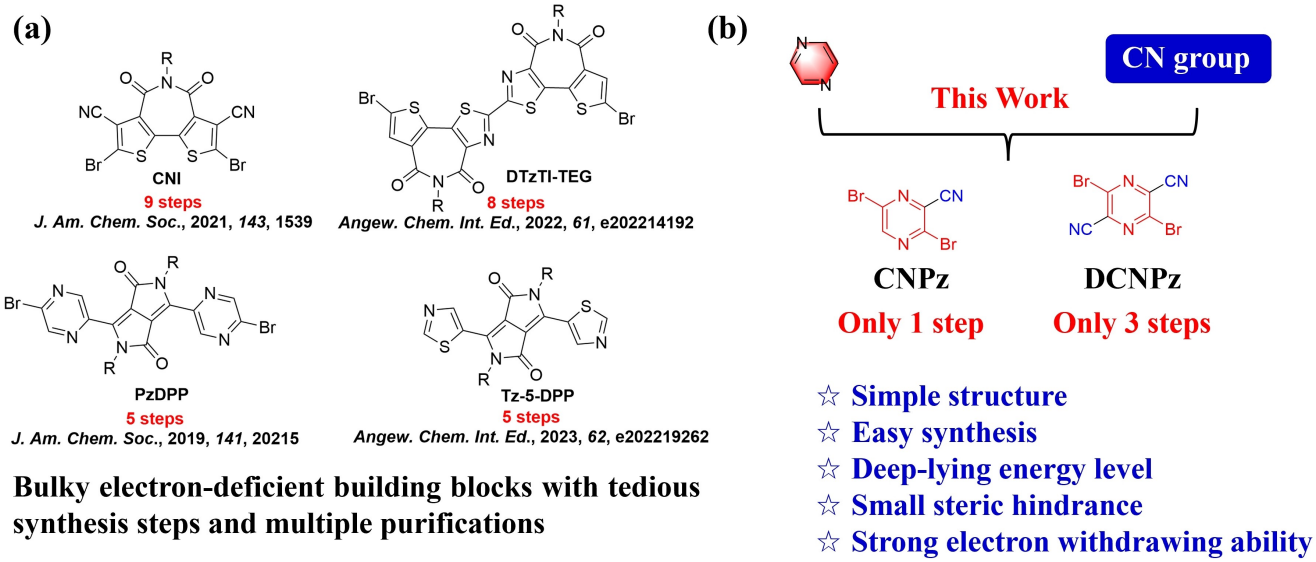

Figure 1. (a) Representative electron-deficient building blocks for n-type organic thermoelectrics materials, which typically require tedious synthesis steps and multiple purifications. (b) The molecular design strategy in this work, which synergistically combines the advantages of both pyrazine and cyano functionalities to achieve novel cyano-functionalized pyrazine building blocks with simple structure and strong electron-withdrawing abilities.

The theoretical calculation was also performed to study the steric hindrance effects of the CN-functionalized pyrazine building blocks (Figure 2). Both CNPz and DCNPz exhibit high planarity, which renders them promising candidates for developing n-type polymer semiconductors. Benefiting from their unique structures, two A–A type polymers, P(DPP-CNPz) and P(DPP-DCNPz) are synthesized. These two polymers show deep-lying FMO energy levels and high planar backbone, which are beneficial to achieving high n-type performance. As a result, substantial unipolar electron mobilities of 0.85 and 1.85 $cm^2V^{-1}s^{-1}$ were obtained for P(DPP-CNPz) and P(DPP-DCNPz) in OTFTs, respectively. Upon doped with molecular dopant *N*-DMBI, P(DPP-CNPz) and P(DPP-DCNPz) display a remarkable σ of 25.30 and 33.93 $S\,cm^{-1}$ with a high PF of 41.4 and 30.4 $\mu W\,m^{-1}K^{-2}$ respectively. These results demonstrate that CNPz and DCNPz are very promising electron-deficient building blocks with simple structures for accessing high-performance and low-cost n-type polymer semiconductors.

Results and Discussion

Synthesis of monomers and polymers:

Asymmetrically functionalized pyrazine of 3,6-dibromopyrazine-2-carbonitrile (CNPz) or symmetrically 3,6-dibromopyrazine-2,5-dicarbonitrile (DCNPz) was synthesized in one step or three steps from 3-aminopyrazinecarbonitrile (Scheme 1a). The detailed synthesis procedure is as follows:

The synthesis of compound **2** was efficiently achieved by oxidation of start material **1** with 3-chloroperbenzoic acid (*m*-CPBA) in 65 % yield. Compound **2** was reacted with trimethylsilyl cyanide (TMSCN) at room temperature for 15 min to get compound **3** in 47 % yield. Subsequently, nitrosation of **3** followed by bromination was realized by treating with *t*-butyl nitrite and copper (II) bromide in acetonitrile at room temperature for 2 h to get target monomer 3,6-dibromopyrazine-2,5-dicarbonitrile (**DCNPz)** in 80 % yield. Their chemical structures were confirmed by ^1H NMR and ^{13}C NMR (Figure S1–S7). The overall yield of CNPz and DCNPz were calculated to be 76 % and 24 %, with a corresponding synthetic cost of \$15.55 g^{-1} and \$68.39 g^{-1} (Table S3–S4).

Then, the two A–A type polymers P(DPP-CNPz) and P(DPP-DCNPz) were synthesized by Stille coupling polymerization of CNPz and DCNPz with the distannylated DPP monomer, respectively. After polymerization, the polymers were purified by successive Soxhlet extraction with methanol, acetone, hexane, dichloromethane, and chloroform to remove oligomers and impurities. The final chlorobenzene fractions were collected and reprecipitated into methanol to get the target polymer for material characterization and device fabrication. The number-average molecular weights (M_n) and polydispersity index (PDI) of two polymers were measured by using high-temperature gel permeation chro-

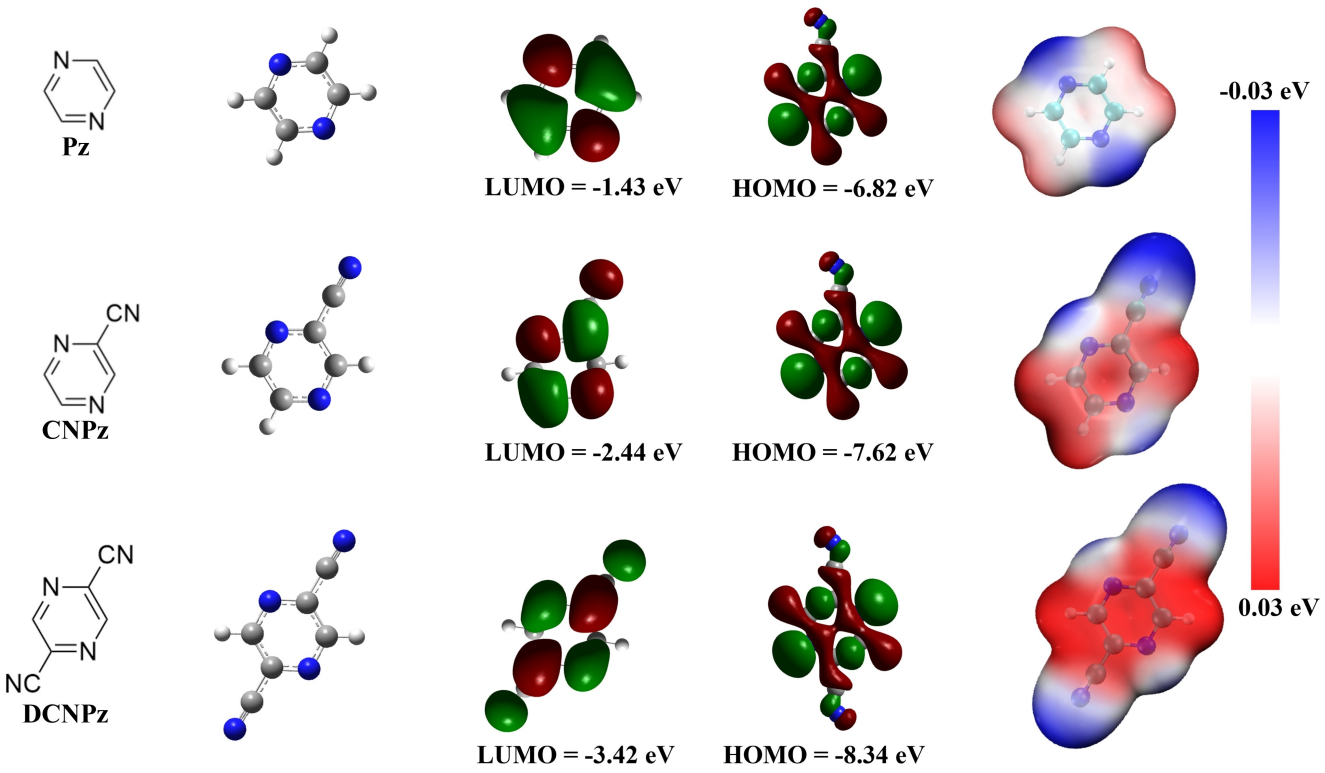

Figure 2. Chemical structures, optimized geometries, frontier molecular orbital energy levels, and electrostatic potential (ESP) surface for pyrazine and the cyano-functionalized pyrazine (CNPz and DCNPz) reported in this work. Calculations are carried out at the DFT//ωB97XD/6-31G(d, p) level.

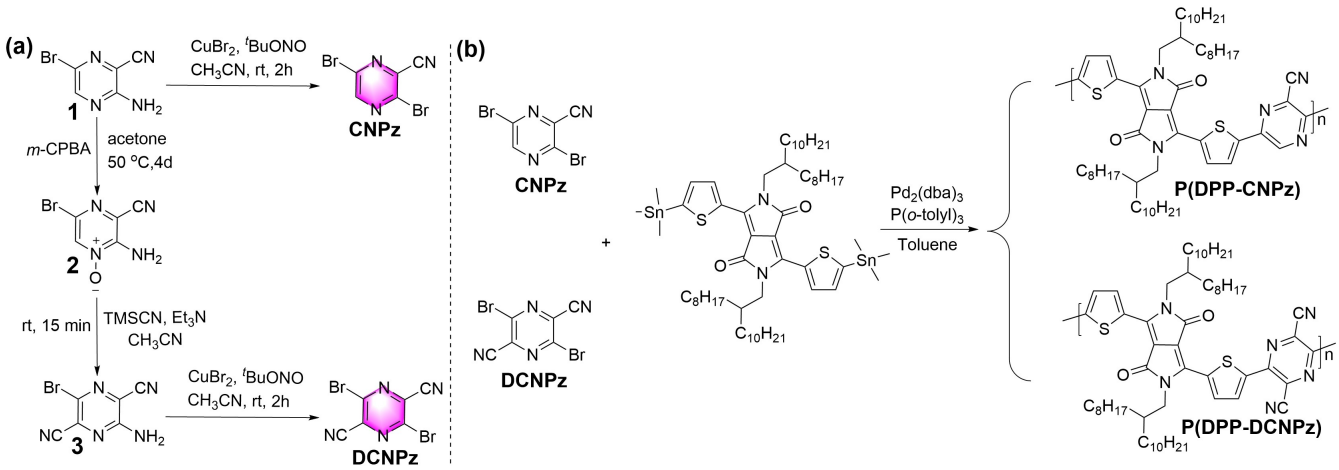

Scheme 1. Synthetic route to (a) dibrominated cyano-functionalized pyrazine monomers CNPz and DCNPz, and (b) their corresponding A–A type polymers P(DPP-CNPz) and P(DPP-DCNPz).

matography (HT-GPC) at 150 °C with 1,2,4-trichlorobenzene as the eluent: P(DPP-CNPz) and P(DPP-DCNPz) showed M_n of 96 and 20 kDa with a PDI of 1.5 and 3.2, respectively (Table 1). Both polymers showed excellent thermal stabilities with decomposition temperatures over 330 °C (Figure S12), and no obvious phase transition can be observed in the temperature range of 30–300 °C (Figure S13).

Theoretical Calculations

To further study the effects of cyano group onto pyrazine-based A–A type polymers, the density functional theory (DFT) calculations were performed at the ωB97XD/6-31G (d, p). In order to simply the calculations, long side chains were replaced with methyl group, and polymers with one repeat unit were calculated. As shown in Figure 3a,b, both polymers showed highly planar backbone, enhancing the intermolecular stacking, which should be beneficial for

Table 1: Molecular Weights, Optical and Electrochemical Properties of P(DPP-CNPz) and P(DPP-DCNPz).

Polymer	M_n (kDa)[a]	PDI[a]	λ_{onset}^{film} (nm)[b]	E_g^{opt} (eV)[c]	E_{LUMO} (eV)[d]	E_{HOMO} (eV)[e]
P(DPP-CNPz)	96	1.5	894	1.38	−3.46	−4.84
P(DPP-DCNPz)	20	3.2	965	1.28	−3.83	−5.11

[a] Determined by GPC using trichlorobenzene as the eluent at 150 °C. [b] Estimated from the absorption edge. [c] Optical band gap (E_g^{opt}) derived from the optical absorption onset of polymer film using the equation: $E_g^{opt} = 1240/\lambda_{onset}^{film}$ (eV). [d] Estimated from cyclic voltammetry measurements. [e] $E_{HOMO} = E_{LUMO} - E_g^{opt}$.

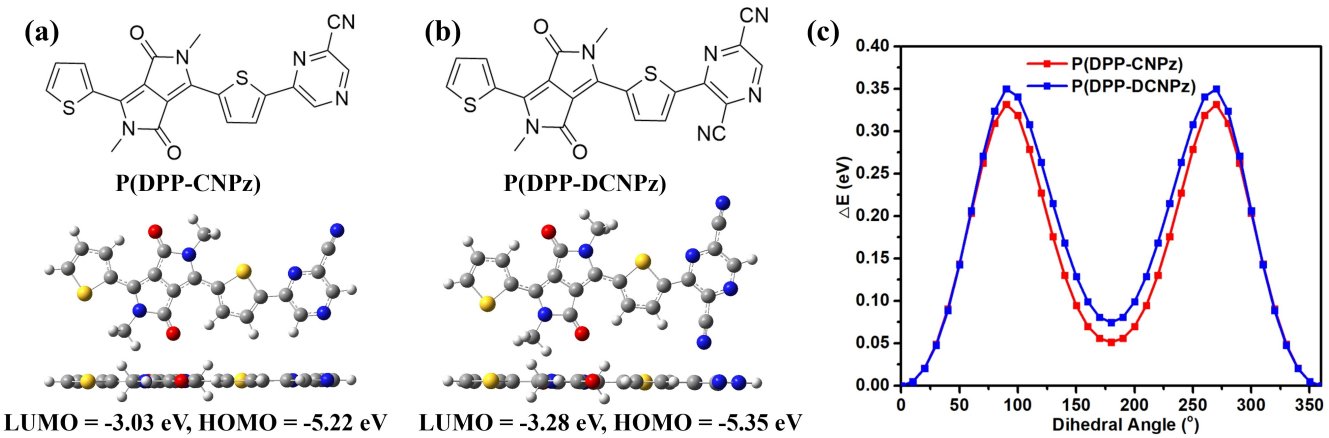

Figure 3. Optimized molecular geometries of P(DPP-CNPz) and P(DPP-DCNPz) by DFT calculation at ωB97XD/6-31G (d, p). Long alkyl side chains were replaced with methyl group to simplify the calculation.

efficient intermolecular charge transport. Although the introduction of cyano group onto pyrazine unit, P(DPP-CNPz) and P(DPP-DCNPz) still exhibit an entirely planar backbone between DPP and neighboring CNPz or DCNPz. For the calculated frontier molecular orbitals (FMOs) energy levels, both low-lying lowest unoccupied molecular orbital (LUMO) and highest occupied molecular orbital (HOMO) energy levels were observed for P(DPP-CNPz) and P(DPP-DCNPz), which can be attributed to the strong electron-withdrawing nature of the cyano-functionalized pyrazine building blocks. In addition, the calculated results also show that the two cyano-functionalized pyrazine-based P(DPP-DCNPz) feature lower- lying LUMO level than one cyano-functionalized pyrazine-based analogue polymer P-(DPP-CNPz). We also calculated the energy barriers for molecular torsions within the polymer backbones (Figure 3c), and large energy barriers were observed for molecular torsion between DPP moiety and CNPz or DCNPz unit, indicating a more rigid backbone for P(DPP-CNPz) and P(DPP-DCNPz). Apparently, the planar backbone of these two polymers should be beneficial for charge transport.

Polymer optical and electrochemical properties

The ultraviolet-visible (UV/Vis) absorption spectra of P-(DPP-CNPz) and P(DPP-DCNPz) in solution and as thin films are shown in Figure 4a, and the corresponding data are summarized in Table 1. In the dilution chloroform solution, P(DPP-CNPz) and P(DPP-DCNPz) exhibited intensive absorption bands in the near-infrared region (800–900 nm) with a typical absorption shoulder for DPP-based polymers.

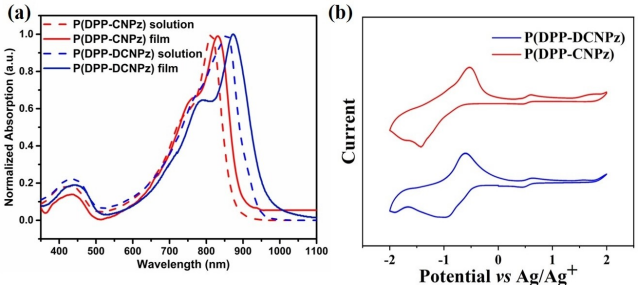

Figure 4. (a) UV/Vis-NIR absorption spectra of P(DPP-CNPz) and P(DPP-DCNPz) in chloroform solution (dash line) and thin-films (solid line), respectively. (b) Cyclic voltammograms curves of polymers P(DPP-CNPz) and P(DPP-DCNPz).

Compared to P(DPP-CNPz), P(DPP-DCNPz) show red-shifted absorption peaks in solution, which likely attributed to the increased intramolecular charge transfer (ICT) character of P(DPP-DCNPz) between DPP unit and strong electron-withdrawing cyano-functionalized pyrazine (DCNPz) unit. In the film state, the absorption peaks of two conjugated polymers also had red-shifted in comparison to those in solution, indicating the compact packing of aggregation in the solid state, probably due to the planar and rigid polymer backbone of these two conjugated polymers. Based on the film absorption onset (λ_{onset}^{film}), the optical band gaps of P(DPP-CNPz) and P(DPP-DCNPz) are calculated to be 1.38 and 1.28 eV, respectively. According to the absorption, the introduction of cyano group into the polymer backbone did not affect the polymer backbone planarity.

Cyclic voltammograms (CV) was used to investigate the electrochemical properties of these two polymers. As shown in Figure 4b, these two polymers display distinctive reduction peaks, indicative of their n-type characteristics. According to their reduction onsets, the LUMO energy levels of P(DPP-CNPz) and P(DPP-DCNPz) were found to be −3.46 and −3.83 eV, respectively. The HOMO energy levels were calculated from the equation $E_{HOMO} = E_{LUMO} - E_g^{opt}$, which are −4.84 and −5.11 eV for P(DPP-CNPz) and P(DPP-DCNPz), respectively. The deep-lying FMOs should facilitate electron injection and suppress hole accumulation, thus leading to unipolar n-type characteristics in OTFT. Additionally, the deep-lying FMOs would also render these two polymers highly desirable in developing high-performance n-type OTE.

Polymer charge transport properties.

The electron-transporting properties of P(DPP-CNPz) and P(DPP-DCNPz) were studied with top-gat/bottom-contact (TG/BC) OTFT device structure. Transfer and output characteristics of the OTFTs are shown in Figure S12, detailed fabrication and characterization procedures are described in the Supporting Information. Both the two A–A type polymers exhibit unipolar n-type electron transporting characteristics with low off current (~10^{-6}–10^{-7} A) and reasonably high on/off ratios ($I_{on}/I_{off} \approx 10^3$–$10^4$), which are due to their extremely low LUMO and HOMO energy levels. The electron mobilities (μ_e) in the linear ($\mu_{e,lin}$) and saturation ($\mu_{e,sat}$) regimes for two polymers were 0.47 and 0.85 $cm^2 V^{-1} s^{-1}$ for P(DPP-CNPz), 0.82 and 1.85 $cm^2 V^{-1} s^{-1}$ for P(DPP-DCNPz), respectively (Table 2). The $\mu_{e,sat}$ of

Table 2: Electron mobilities of pristine polymers and electrical conductivities and power factors of *N*-DMBI doped polymers.

Polymer	$\mu_{e,lin}$ ($cm^2 V^{-1} s^{-1}$)	$\mu_{e,sat}$ ($cm^2 V^{-1} s^{-1}$)	σ[a] ($S cm^{-1}$)	S[b] ($\mu V K^{-1}$)	PF[b] ($\mu W m^{-1} K^{-2}$)
P(DPP-CNPz)	0.47	0.85	25.30	−131.9	41.4
P(DPP-DCNPz)	0.82	1.85	33.93	−95.25	30.4

[a]The best electrical conductivity performance of these two polymers at their optimal *N*-DMBI dopant concentrations. [b] The best power factor performance
of these polymers and the corresponding Seebeck coefficient factor values.

$1.85\ cm^2V^{-1}s^{-1}$ is much higher than recently reported polymer PCNDFDE-DPP.[24] Compared with other DPP-based copolymers, which typically show p-type or ambipolar transport behaviors, P(DPP-CNPz) and P(DPP-DCNPz) polymers only show unipolar n-type charge transport in OTFT. The result demonstrates that cyano-functionalized pyrazine (CNPz or DCNPz) is a strong electron-withdrawing building block for constructing unipolar n-type polymer semiconductors.

n-Doping Thermoelectric Performances

The deep-lying LUMOs of P(DPP-CNPz) and P(DPP-DCNPz) should be beneficial for efficient n-type doping. *N*-DMBI was selected to dope both polymers because of its strong n-doping ability and good solution processability. UV/Vis-NIR absorption spectroscopy was conducted to evaluate the n-doping efficiency for both polymers (Figure 5a,b). Upon doping, P(DPP-CNPz) and P(DPP-DCNPz) films are accompanied by a sharp decrease in the band intensity at ≈800 nm, along with a new feature peak at 1300–2300 nm are appearing, respectively. These new spectral features are attributed to the polaron/bipolaron-induced transitions, in accord with previous studies. Note that P(DPP-DCNPz) shows a stronger polaron or bipolaron absorption intensity than P(DPP-CNPz) for each dopant fraction. All the results suggest that P(DPP-DCNPz) can be more easily doped than P(DPP-CNPz). This result was further supported by electron spinning resonance (ESR) measurements (Figure 5c). As expected, due to its lower LUMO level, higher intensity of radical signal was observed for P(DPP-DCNPz) than P(DPP-CNPz), suggesting an increased charge concentration of the doped P(DPP-DCNPz) film, which should contribute to a higher electrical conductivity of this polymer.

Thermoelectric properties of polymers

The thermoelectric performances of doped polymers were evaluated by measuring the electrical conductivities and Seebeck coefficients. As shown in Figure 6 and summarized in Table 2. The maximum σ values of P(DPP-CNPz) and P(DPP-DCNPz) are 25.3 and 33.9 $S\,cm^{-1}$, respectively, which obtained at a dopant concentration of 2.0 $mg\,mL^{-1}$ for P(DPP-CNPz) and 1.2 $mg\,mL^{-1}$ for P(DPP-DCNPz). The trend in σ_{max} is consistent with the trend in the $\mu_{e,OTFT}$ for these two polymers. Further increased the *N*-DMBI dopant concentration resulted in a decreased in σ, this maybe because the excessive dopants disrupt polymer morphology and lower the polymer crystallinity. The higher σ value of P(DPP-DCNPz) should be attributed to its relatively lower-lying LUMO, higher $\mu_{e,OTFT}$ and higher n-doping efficiency as revealed by the ESR studies.

Then we estimated the Seebeck coefficients (*S*) of both doped films. As shown in Figure 6a,b, all the *S* values are negative, confirming n-type doping. As the doping level

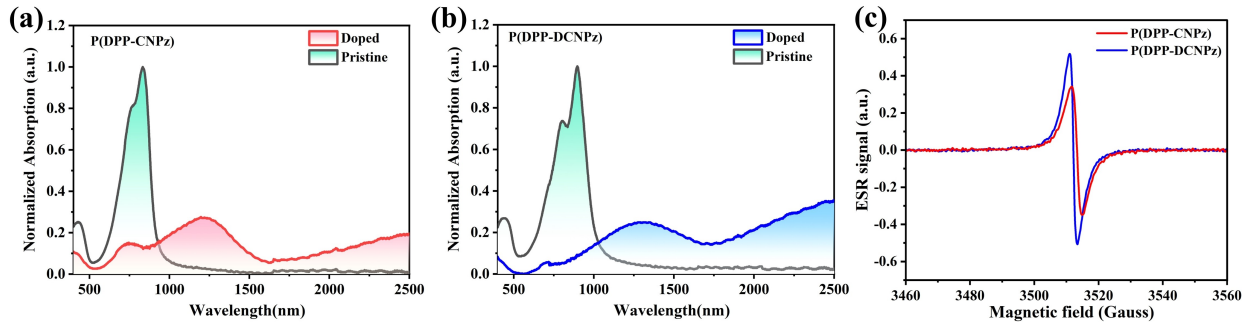

Figure 5. UV/Vis-NIR absorption spectra of the thin films of (a) P(DPP-CNPz) and (b) P(DPP-DCNPz) before and after n-doping with the molecular dopant *N*-DMBI. (c) ESR signals of P(DPP-CNPz) and P(DPP-DCNPz) after n-doping with *N*-DMBI.

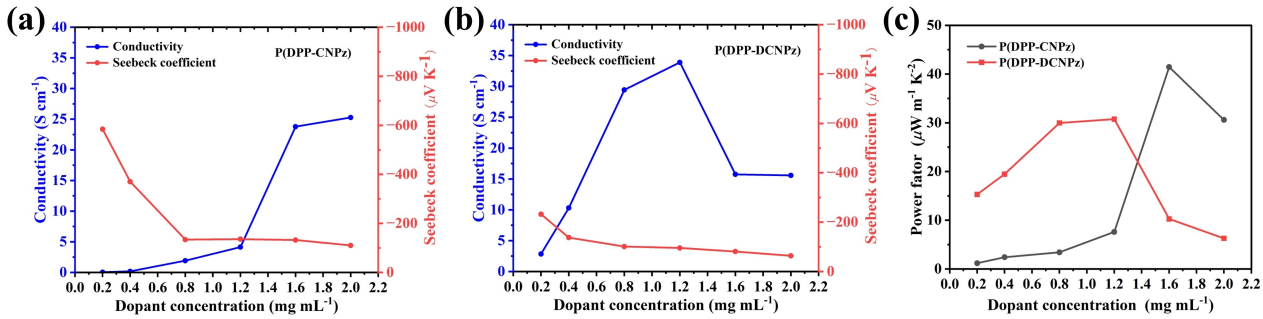

Figure 6. Electrical conductivity and Seebeck coefficient of (a) P(DPP-CNPz) and (b) P(DPP-DCNPz), and (c) the corresponding power factors upon doping with *N*-DMBI solution (0.2–2.0 $mg\,mL^{-1}$).

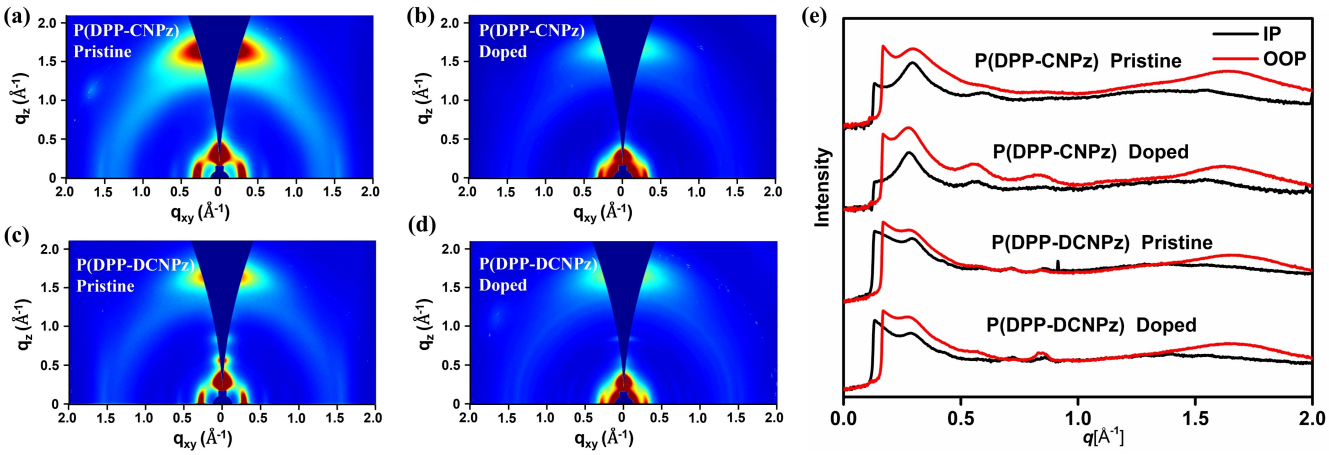

Figure 7. 2D GIWAXS images of (a,b) P(DPP-CNPz) and (c,d) P(DPP-DCNPz) films before (a,c) and after (b,d) doped by *N*-DMBI, and (e) in-plane and out-of-plane line-cut profiles of the 2D-GIWAXS images.

increased, the S value of P(DPP-CNPz) decreased from -584 to $-110\,\mu V\,K^{-1}$. For P(DPP-DCNPz), S varied from -232 to $-63\,\mu V\,K^{-1}$. The S was consistent with its negative correlation with the charge carrier concentration. The power factors (PF) of doped polymer films were calculated with the formula of $PF=\sigma S^2$ (Figure 6c). The best PF values for P(DPP-CNPz) and P(DPP-DCNPz) are 41.4 and $30.4\,\mu W\,m^{-1}\,K^{-2}$, respectively (Table 2). Please note that the PFs recorded for P(DPP-CNPz) and P(DPP-DCNPz) are among the highest values reported for n-type OTE materials, which are also much higher than other DPP-based polymers.[25] This result suggests that the introduction of CNPz or DCNPz electron-deficient building blocks onto the polymer backbone is an efficient strategy for organic thermoelectric application.

Film Morphology and Microstructure.

Atomic force microscopy (AFM) was performed to investigate the surface morphology properties of both pristine and doped films of P(DPP-CNPz) and P(DPP-DCNPz) (Figure S17–18). All the pristine films show smooth surfaces with root mean square (RMS) roughnesses of 0.89 and 0.65 nm for P(DPP-CNPz) and P(DPP-DCNPz), respectively. The smaller RMS value of P(DPP-DCNPz) should be responsible for its higher electron mobility in OTFT. After doping with *N*-DMBI, rougher surface with larger RMS were found for both polymer films, 2.49 nm for P(DPP-CNPz) and 1.55 nm for P(DPP-DCNPz). The larger RMS values may be caused by the aggregation of dopant on the film surface. However, a relatively smaller RMS roughness of doped P(DPP-DCNPz) film might suggest its better miscibility with *N*-DMBI dopant. The good miscibility of the P(DPP-DCNPz)/*N*-DMBI blend improved doping efficiency, thus resulting in an enhanced conductivity.

To gain insights into polymer chain packing of P(DPP-CNPz) and P(DPP-DCNPz) before and after *N*-DMBI doping, grazing-incidence wide-angle X-ray scattering (GIWAXS) was carried out, the 2D-GIWAXS images and one-dimensional line profiles are showed in Figure 7. Clearly, both pristine polymers show preferential face-on orientation with strong out-of-plane (OOP) (010) π-stacking diffraction peak. Based on the q_z values of (100)/(010) diffraction peaks, the lamellar stacking/π-stacking distances of P(DPP-CNPz) and P(DPP-DCNPz) polymers were calculated to be 20.9/3.80 Å and 21.6/3.76 Å, respectively. After doping, from the GIWAXS, the in-plane lamellar reflections nearly no obvious change in intensity, however, in the out-of-plane direction, (100), (200), and (300) lamellar reflections increase in intensity. Also, we find that the diffraction patterns and π-stacking distances remain almost unchanged in OOP directions for the two polymers, implying the highly ordered molecular packing was well maintained during the doping process. These results indicated that the dopants are mainly distributed in the amorphous region of polymer films. Clearly, these microstructure characteristics of polymers in both pristine and n-doped films should be responsible for their high electron mobility and high TE performance.

Conclusion

In summary, we have designed and synthesized two simple structured highly electron-deficient building blocks, CNPz and DCNPz, by incorporating strong electron-withdrawing CN groups into electron-deficient pyrazine backbone. The new building blocks not only feature easy synthesis and preparation procedures (one step for CNPz and three steps for DCNPz) but also show small steric hindrance, planar backbone and high electron-deficient characteristics, rendering them ideal candidates for constructing low-cost n-type polymer semiconductors. Benefiting from their strong electron-withdrawing ability of CNPz and DCNPz, the resulting polymers P(DPP-CNPz) and P(DPP-DCNPz) exhibited unipolar n-type transport characteristics with μ_e of 0.85 and $1.85\,cm^2\,V^{-1}\,s^{-1}$ achieved in OTFT devices, respectively.

After n-doping with molecular dopant *N*-DMBI, P(DPP-CNPz) and P(DPP-DCNPz) exhibited electrical conductivities and power factors of 25.3 $S\,cm^{-1}$ and 41.4 $\mu W\,m^{-1}K^{-2}$, and 33.9 $S\,cm^{-1}$ and 30.4 $\mu W\,m^{-1}K^{-2}$, respectively. These values are among the highest reported for n-type OTE materials. This work demonstrates that the incorporation of simple structured cyano-functionalized pyrazine electron-deficient building blocks into the polymer backbone is an efficient strategy to greatly lower the LUMO energy levels of conjugated polymers and offers new insights into material design guidelines for the future development of n-type organic electronics.

Acknowledgements

Y. Shi thanks the National Natural Science Foundation of China (No. 22105004), Anhui Provincial Natural Science Foundation (No. 2308085Y15), Wuhu Science and Technology Plan Project (2023jc15) for supporting this work.

Conflict of Interest

The authors declare no conflict of interest.

Data Availability Statement

The data that support the findings of this study are available in the supplementary material of this article.

Keywords: n-type organic thermoelectrics · electron-deficient building block · cyano-functionalized pyrazine · acceptor-acceptor polymers · electrical conductivities

[1] a) X. Guo, A. Facchetti, T. J. Marks, *Chem. Rev.* **2014**, *114*, 8943–9021; b) N. Liang, D. Meng, Z. Wang, *Acc. Chem. Res.* **2021**, *54*, 961–975; c) J. Zaumseil, H. Sirringhaus, *Chem. Rev.* **2007**, *107*, 1296–1323; d) Y. Teshima, M. Saito, T. Mikie, K. Komeyama, I. Osaka, *Macromolecules* **2021**, *54*, 3489–3497.

[2] a) C. Yan, S. Barlow, Z. Wang, H. Yan, A. K. Y. Jen, S. R. Marder, X. Zhan, *Nat. Rev. Mater.* **2018**, *3*, 18003; b) J. Zhang, H. S. Tan, X. Guo, A. Facchetti, H. Yan, *Nat. Energy* **2018**, *3*, 720–731; c) L. Meng, Y. Zhang, X. Wan, C. Li, X. Zhang, Y. Wang, X. Ke, Z. Xiao, L. Ding, R. Xia, H. L. Yip, Y. Cao, Y. Chen, *Science* **2018**, *361*, 1094–1098.

[3] a) X. Yu, D. Gao, Z. Li, X. Sun, B. Li, Z. Zhu, Z. a. Li, *Angew. Chem. Int. Ed.* **2023**, *62*, e202218752; b) T. Niu, W. Zhu, Y. Zhang, Q. Xue, X. Jiao, Z. Wang, Y. M. Xie, P. Li, R. Chen, F. Huang, Y. Li, H. L. Yip, Y. Cao, *Joule* **2021**, *5*, 249–269; c) N. Wang, K. Zhao, T. Ding, W. Liu, A. S. Ahmed, Z. Wang, M. Tian, X. W. Sun, Q. Zhang, *Adv. Energy Mater.* **2017**, *7*, 1700522.

[4] a) J. Ding, Z. Liu, W. Zhao, W. Jin, L. Xiang, Z. Wang, Y. Zeng, Y. Zou, F. Zhang, Y. Yi, Y. Diao, C. R. McNeill, C. a. D. Di, D. Zhang, D. Zhu, *Angew. Chem. Int. Ed.* **2019**, *58*, 18994–18999; b) C. J. Yao, H. L. Zhang, Q. Zhang, *Polymer* **2019**, *11*, 107; c) D. Yuan, D. Huang, S. M. Rivero, A. Carreras, C. Zhang, Y. Zou, X. Jiao, C. R. McNeill, X. Zhu, C. a. Di, D. Zhu, D. Casanova, J. Casado, *Chem* **2019**, *5*, 964–976; d) K. Xu, H. Sun, T. P. Ruoko, G. Wang, R. Kroon, N. B. Kolhe, Y. Puttisong, X. Liu, D. Fazzi, K. Shibata, C. Y. Yang, N. Sun, G. Persson, A. B. Yankovich, E. Olsson, H. Yoshida, W. M. Chen, M. Fahlman, M. Kemerink, S. A. Jenekhe, C. Müller, M. Berggren, S. Fabiano, *Nat. Mater.* **2020**, *19*, 738–744; e) S. Jhulki, H.-I. Un, Y.-F. Ding, C. Risko, S. K. Mohapatra, J. Pei, S. Barlow, S. R. Marder, *Chem* **2021**, *7*, 1050–1065; f) Y. Lu, J.-Y. Wang, J. Pei, *Acc. Chem. Res.* **2021**, *54*, 2871–2883; g) Y. Zeng, W. Zheng, Y. Guo, G. Han, Y. Yi, *J. Mater. Chem. A* **2020**, *8*, 8323–8328; h) Z. Liu, Y. Hu, P. Li, J. Wen, J. He, X. Gao, *J. Mater. Chem. C* **2020**, *8*, 10859–10867; i) D. Wang, L. Liu, X. Gao, C.-a. Di, D. Zhu, *CCS Chem.* **2021**, *3*, 2212–2225.

[5] a) B. Sun, W. Hong, Z. Yan, H. Aziz, Y. Li, *Adv. Mater.* **2014**, *26*, 2636–2642; b) G. Kim, S.-J. Kang, G. K. Dutta, Y.-K. Han, T. J. Shin, Y.-Y. Noh, C. Yang, *J. Am. Chem. Soc.* **2014**, *136*, 9477–9483; c) T. Duan, W. Feng, Y. Li, Z. Li, Z. Zhang, H. Liang, H. Chen, C. Zhong, S. Jeong, C. Yang, S. Chen, S. Lu, O. A. Rakitin, C. Li, X. Wan, B. Kan, Y. Chen, *Angew. Chem. Int. Ed.* **2023**, *62*, e202308832; d) B. Pang, C. Liao, X. Xu, L. Yu, R. Li, Q. Peng, *Adv. Mater.* **2023**, *35*, 2300631; e) Y. Shao, Y. Gao, R. Sun, M. Zhang, J. Min, *Adv. Mater.* **2023**, *35*, 2208750.

[6] a) J. Liu, G. Ye, B. v. d. Zee, J. Dong, X. Qiu, Y. Liu, G. Portale, R. C. Chiechi, L. J. A. Koster, *Adv. Mater.* **2018**, *30*, 1804290; b) S. Wang, H. Sun, T. Erdmann, G. Wang, D. Fazzi, U. Lappan, Y. Puttisong, Z. Chen, M. Berggren, X. Crispin, A. Kiriy, B. Voit, T. J. Marks, S. Fabiano, A. Facchetti, *Adv. Mater.* **2018**, *30*, 1801898; c) Y. Lu, Z. D. Yu, R. Z. Zhang, Z. F. Yao, H. Y. You, L. Jiang, H. I. Un, B. W. Dong, M. Xiong, J. Y. Wang, J. Pei, *Angew. Chem. Int. Ed.* **2019**, *58*, 11390–11394; d) D. Huang, H. Yao, Y. Cui, Y. Zou, F. Zhang, C. Wang, H. Shen, W. Jin, J. Zhu, Y. Diao, W. Xu, C. Di, D. Zhu, *J. Am. Chem. Soc.* **2017**, *139*, 13013–13023; e) O. Bardagot, P. Kubik, T. Marszalek, P. Veyre, A. A. Medjahed, M. Sandroni, B. Grévin, S. Pouget, T. Nunes Domschke, A. Carella, S. Gambarelli, W. Pisula, R. Demadrille, *Adv. Funct. Mater.* **2020**, *30*, 2000449; f) J. Duan, J. Ding, D. Wang, X. Zhu, J. Chen, G. Zhu, C. Chen, Y. Yu, H. Liao, Z. Li, C.-a. Di, W. Yue, *Adv. Sci.* **2023**, *10*, 2204872; g) Y. Song, J. Ding, X. Dai, C. Li, C.-a. Di, D. Zhang, *ACS Materials Lett.* **2022**, 521–527; h) H. Tang, Y. Liang, C. Liu, Z. Hu, Y. Deng, H. Guo, Z. Yu, A. Song, H. Zhao, D. Zhao, Y. Zhang, X. Guo, J. Pei, Y. Ma, Y. Cao, F. Huang, *Nature* **2022**, *611*, 271–277; i) H. Guo, C.-Y. Yang, X. Zhang, A. Motta, K. Feng, Y. Xia, Y. Shi, Z. Wu, K. Yang, J. Chen, Q. Liao, Y. Tang, H. Sun, H. Y. Woo, S. Fabiano, A. Facchetti, X. Guo, *Nature* **2021**, *599*, 67–73.

[7] a) Z. Fan, P. Li, D. Du, J. Ouyang, *Adv. Energy Mater.* **2017**, *7*, 1602116; b) X. Wang, X. Zhang, L. Sun, D. Lee, S. Lee, M. Wang, J. Zhao, Y. Shao-Horn, M. Dincă, T. Palacios, K. K. Gleason, *Sci. Adv.* **2018**, *4*, eaat5780.

[8] a) V. Vijayakumar, Y. Zhong, V. Untilova, M. Bahri, L. Herrmann, L. Biniek, N. Leclerc, M. Brinkmann, *Adv. Energy Mater.* **2019**, *9*, 1900266; b) K. Shi, F. Zhang, C.-A. Di, T.-W. Yan, Y. Zou, X. Zhou, D. Zhu, J.-Y. Wang, J. Pei, *J. Am. Chem. Soc.* **2015**, *137*, 6979–6982; c) W. Xing, S. Wu, Y. Liang, Y. Sun, Y. Zou, L. Liu, W. Xu, D. Zhu, *ACS Appl. Mater. Interfaces* **2020**, *12*, 29540–29548; d) J. Han, H. Fan, Q. Zhang, Q. Hu, T. P. Russell, H. E. Katz, *Adv. Funct. Mater.* **2005**, *31*, 2005901.

[9] a) R. Kroon, D. Kiefer, D. Stegerer, L. Yu, M. Sommer, C. Müller, *Adv. Mater.* **2017**, *29*, 1700930; b) D. Kiefer, A. Giovannitti, H. Sun, T. Biskup, A. Hofmann, M. Koopmans, C. Cendra, S. Weber, L. J. Anton Koster, E. Olsson, J. Rivnay, S. Fabiano, I. McCulloch, C. Müller, *ACS Energy Lett.* **2018**, *3*, 278–285; c) S. E. Yoon, S. J. Shin, S. Y. Lee, G. G. Jeon, H. Kang, H. Seo, J. Zheng, J. H. Kim, *ACS Appl. Polym. Mater.* **2020**, *2*, 2729–2735; d) J. Wang, L. Liu, F. Wu, Z. Liu, Z. Fan,

L. Chen, Y. Chen, *ChemSusChem* **2022**, *15*, e202102420; e) A. Marks, X. Chen, R. Wu, R. B. Rashid, W. Jin, B. D. Paulsen, M. Moser, X. Ji, S. Griggs, D. Meli, X. Wu, H. Bristow, J. Strzalka, N. Gasparini, G. Costantini, S. Fabiano, J. Rivnay, I. McCulloch, *J. Am. Chem. Soc.* **2022**, *144*, 4642–4656; f) T. L. D. Tam, M. Lin, S. W. Chien, J. Xu, *ACS Macro Lett.* **2021**, 110–115.

[10] a) Y. Wang, H. Guo, A. Harbuzaru, M. A. Uddin, I. Arrechea-Marcos, S. Ling, J. Yu, Y. Tang, H. Sun, J. T. López Navarrete, R. P. Ortiz, H. Y. Woo, X. Guo, *J. Am. Chem. Soc.* **2018**, *140*, 6095–6108; b) T. Okamoto, S. Kumagai, E. Fukuzaki, H. Ishii, G. Watanabe, N. Niitsu, T. Annaka, M. Yamagishi, Y. Tani, H. Sugiura, T. Watanabe, S. Watanabe, J. Takeya, *Sci. Adv.* **2020**, *6*, eaaz0632; c) D. Tu, Q. Yang, S. Yu, X. Guo, C. Li, *Chem. Sci.* **2021**, *12*, 2848–2852; d) P. Cheng, X. Zhao, X. Zhan, *Acc. Mater. Res.* **2022**, *3*, 309–318; e) H. Xin, B. Hou, X. Gao, *Acc. Chem. Res.* **2021**, *54*, 1737–1753; f) Y. Shi, W. Li, X. Wang, L. Tu, M. Li, Y. Zhao, Y. Wang, Y. Liu, *Chem. Mater.* **2022**, *34*, 1403–1413.

[11] A. Pron, M. Leclerc, *Prog. Polym. Sci.* **2013**, *38*, 1815–1831.

[12] K. Feng, J. Huang, X. Zhang, Z. Wu, S. Shi, L. Thomsen, Y. Tian, H. Y. Woo, C. R. McNeill, X. Guo, *Adv. Mater.* **2020**, *32*, 2001476.

[13] a) C. Dong, S. Deng, B. Meng, J. Liu, L. Wang, *Angew. Chem. Int. Ed.* **2021**, *60*, 16184–16190; b) X. Long, Z. Ding, C. Dou, J. Zhang, J. Liu, L. Wang, *Adv. Mater.* **2016**, *28*, 6504–6508; c) J. Xu, Y. Zhang, J. Liu, L. Wang, *Angew. Chem. Int. Ed.* **2023**, *62*, e202310838; d) Y. Min, C. Dou, D. Liu, H. Dong, J. Liu, *J. Am. Chem. Soc.* **2019**, *141*, 17015–17021.

[14] a) Y. Shi, H. Guo, M. Qin, J. Zhao, Y. Wang, H. Wang, Y. Wang, A. Facchetti, X. Lu, X. Guo, *Adv. Mater.* **2018**, *30*, 1705745; b) Y. Shi, H. Guo, M. Qin, Y. Wang, J. Zhao, H. Sun, H. Wang, Y. Wang, X. Zhou, A. Facchetti, X. Lu, M. Zhou, X. Guo, *Chem. Mater.* **2018**, *30*, 7988–8001; c) Y. Shi, H. Guo, J. Huang, X. Zhang, Z. Wu, K. Yang, Y. Zhang, K. Feng, H. Y. Woo, R. Ortiz, M. Zhou, X. Guo, *Angew. Chem. Int. Ed.* **2020**, *59*, 14449–14457; d) Y. Wang, T. Hasegawa, H. Matsumoto, T. Michinobu, *Angew. Chem. Int. Ed.* **2019**, *58*, 11893–11902.

[15] a) X. Guo, M. D. Watson, *Org. Lett.* **2008**, *10*, 5333–5336; b) H. Yan, Z. Chen, Y. Zheng, C. Newman, J. R. Quinn, F. Dötz, M. Kastler, A. Facchetti, *Nature* **2009**, *457*, 679–686.

[16] a) Y. Wang, M. Nakano, T. Michinobu, Y. Kiyota, T. Mori, K. Takimiya, *Macromolecules* **2017**, *50*, 857–864; b) Y. Wang, K. Takimiya, *Adv. Mater.* **2020**, *32*, 2002060.

[17] a) T. Lei, J. H. Dou, X. Y. Cao, J. Y. Wang, J. Pei, *J. Am. Chem. Soc.* **2013**, *135*, 12168–12171; b) Z. D. Yu, Y. Lu, Z. Y. Wang, H. I. Un, S. J. Zelewski, Y. Cui, H. Y. You, Y. Liu, K. F. Xie, Z. F. Yao, Y. C. He, J. Y. Wang, W. B. Hu, H. Sirringhaus, J. Pei, *Sci. Adv.* **2023**, *9*, eadf3495.

[18] Y. Shi, X. Zhang, T. Du, Y. Han, Y. Deng, Y. Geng, *Angew. Chem. Int. Ed.* **2023**, *62*, e202219262.

[19] K. Feng, H. Guo, J. Wang, Y. Shi, Z. Wu, M. Su, X. Zhang, J. H. Son, H. Y. Woo, X. Guo, *J. Am. Chem. Soc.* **2021**, *143*, 1539–1552.

[20] a) M. Xiong, X. Yan, J.-T. Li, S. Zhang, Z. Cao, N. Prine, Y. Lu, J.-Y. Wang, X. Gu, T. Lei, *Angew. Chem. Int. Ed.* **2021**, *60*, 8189–8197; b) X. Yan, M. Xiong, X.-Y. Deng, K.-K. Liu, J.-T. Li, X.-Q. Wang, S. Zhang, N. Prine, Z. Zhang, W. Huang, Y. Wang, J.-Y. Wang, X. Gu, S. K. So, J. Zhu, T. Lei, *Nat. Commun.* **2021**, *12*, 5723; c) X. Yan, M. Xiong, J. T. Li, S. Zhang, Z. Ahmad, Y. Lu, Z. Y. Wang, Z. F. Yao, J. Y. Wang, X. Gu, T. Lei, *J. Am. Chem. Soc.* **2019**, *141*, 20215–20221.

[21] a) Y. Shi, J. Li, H. Sun, Y. Li, Y. Wang, Z. Wu, S. Y. Jeong, H. Y. Woo, S. Fabiano, X. Guo, *Angew. Chem. Int. Ed.* **2022**, *61*, e202214192; b) J. Li, M. Liu, K. Yang, Y. Wang, J. Wang, Z. Chen, K. Feng, D. Wang, J. Zhang, Y. Li, H. Guo, Z. Wei, X. Guo, *Adv. Funct. Mater.* **2023**, *33*, 2213911.

[22] X. Chen, Z. Zhang, Z. Ding, J. Liu, L. Wang, *Angew. Chem. Int. Ed.* **2016**, *55*, 10376–10380.

[23] a) D. Yuan, W. Liu, X. Zhu, *Chem. Soc. Rev.* **2023**, *52*, 3842–3872; b) T. L. D. Tam, J. Xu, *J. Mater. Chem. C* **2020**, *8*, 17261–17268; c) S. Deng, C. Dong, J. Liu, B. Meng, J. Hu, Y. Min, H. Tian, J. Liu, L. Wang, *Angew. Chem. Int. Ed.* **2023**, *62*, e202216049; d) H. Wang, C. Yu, *Joule* **2019**, *3*, 53–80.

[24] J. Li, Z. Chen, J. Wang, S. Y. Jeong, K. Yang, K. Feng, J. Yang, B. Liu, H. Y. Woo, X. Guo, *Angew. Chem. Int. Ed.* **2023**, *62*, e202307647.

[25] H. Zeng, M. Mohammed, V. Untilova, O. Boyron, N. Berton, P. Limelette, B. Schmaltz, M. Brinkmann, *Adv. Electron. Mater.* **2021**, *7*, 2000880.

Manuscript received: December 19, 2023
Accepted manuscript online: January 24, 2024
Version of record online: February 6, 2024